THE JOURNAL OF PHYSICAL CHEMISTRY C

pubs.acs.org/JPCC Article

Colloidal Bimetallic Nanorings for Strong Plasmon Exciton Coupling

C. Meric Guvenc, Fadime Mert Balci, Sema Sarisozen, Nahit Polat, and Sinan Balci*

Cite This: J. Phys. Chem. C 2020, 124, 8334−8340 Read Online

ACCESS | Metrics & More | Article Recommendations | Supporting Information

ABSTRACT: Nobel-metal nanostructures strongly localize and manipulate light at nanoscale dimension by supporting surface plasmon polaritons. In fact, the optical properties of the nobel-metal nanostructures strongly depend on their morphology and composition. Until now, various metal nanostructures such as nanocubes, nanoprisms, nanorods, and recently hollow nanostructures have been demonstrated. In addition, the plasmonic field can be further enhanced at nanoparticle dimers and aggregates because of highly localized and intense optical fields, which is known as "plasmonic hot spots". However, colloidally synthesized and circular-shaped nanoring nanostructures with plasmonic hot spots are still lacking. We, herein, show for the first time that colloidal bimetallic nanorings with plasmonic nanocavities and tunable plasmon resonance wavelengths can be synthesized via colloidal synthesis and galvanic replacement reactions. In addition, in the strong coupling regime, plasmons in nanorings and excitons in J-aggregates interact strongly and nanoring-shaped colloidal plexcitonic nanoparticles are demonstrated. The results reveal that the optical properties of the nanoring and the onset of strong coupling can be tamed by the galvanic replacement reaction. Further, the plasmonic nanocavity in the nanorings has immense potential for applications in sensing and spectroscopy because of the space, enclosed by the plasmonic nanocavity, is empty and accessible to a variety of molecules, ions, and quantum dots.

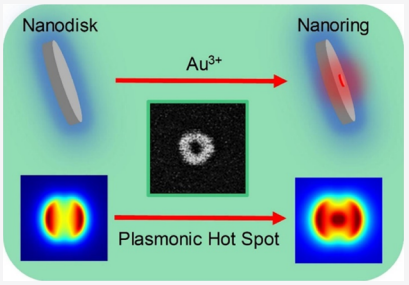

INTRODUCTION

Metallic nanoparticles have attracted a tremendous amount of interest, owing to their extraordinary optical properties caused by their localized surface plasmon polaritons (SPP).[1] Metallic nanoparticles are cavities or tiny antennas at the nanoscale dimension. They enable strong localization and guidance of optical fields. The plasmonic field can be further enhanced at nanoparticle dimers and aggregates because of highly localized and intense optical fields at the nanoparticle−nanoparticle junctions, which is known as "plasmonic hot spots".[2] The plasmonic hot spots have been used to enhance fluorescence of dye molecules or quantum dots,[3] and Raman scattering of molecules, and to demonstrate single-molecule strong coupling as well.[4,5] In fact, the optical properties of metallic nanostructures strongly depend on their geometry, size, composition, and dielectric environment.[6] Until now, various metallic nanostructures such as nanocubes,[7] triangular nanoprisms,[8] nanorods,[9] nanodisks,[10] nanostars,[11] and hollow nanostructures[12,13] have been demonstrated by various techniques. Among them, colloidal synthesis of metal nanoparticles is very attractive because large quantities of metal nanoparticles can be synthesized; no specialized instrumentation is required; size and shape of the nanoparticles can be easily controlled by playing around with the reaction ingredients such as metal ions, reducing agents, and capping agents.[14] The metallic hollow nanoparticles including nanoframes,[15,16] nanocages,[17] and nanorings[18−20] are a relatively new class of metallic nanostructures with tunable plasmon resonance wavelengths. For example, Lin et al. reported synthesis of gold nanoframes and nanorings by first depositing gold on silver nanotemplates and then selectively etching the silver layer.[15] In another study, colloidal synthesis of gold- and silver-alloyed triangular nanoframes was reported.[21] Also, Krishnan et al. converted silver nanoplates to silver−gold nanodisks by galvanic replacement-deposition reactions and, consequently, enormously improved the stability of bimetallic nanodisks.[22] Additionally, lithographic techniques have been used for fabricating hollow metallic nanostructures.[19,23] Previously reported approaches for the synthesis of hollow metal nanostructures require (i) special instrumentation,[19] (ii) etching and metal deposition steps,[15] (iii) limited control over the size and geometry of the hollow in the nanostructures, (iv) high temperature,[24] and (vi) reactions involving gold ions and a reducer (e.g., formaldehyde),[25] which make them impractical for many plasmonic applications. In fact, colloidally synthesized and truly circular-shaped nanoring nanostructures with tunable plasmon resonance and plasmonic nanocavities are still lacking.

In the weak coupling regime, metal nanoparticles interact weakly with a molecular transition or electron−hole pairs, namely excitons, and emission of molecules or semiconductor quantum dots are greatly modified with respect to the free space

Received: February 5, 2020
Revised: March 30, 2020
Published: March 31, 2020

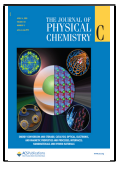

https://dx.doi.org/10.1021/acs.jpcc.0c01011
J. Phys. Chem. C 2020, 124, 8334−8340

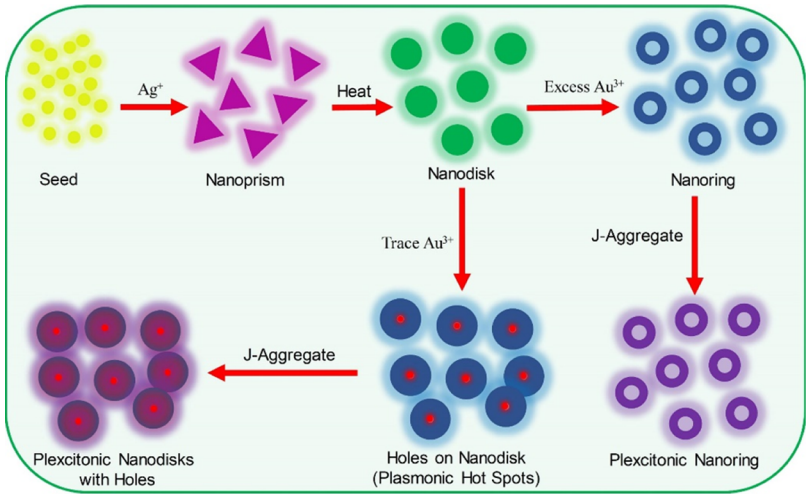

Figure 1. Shape engineering of plasmonic nanoparticles. The scheme represents synthesis of plexcitonic nanorings. When the inner diameter of the nanoring is small, plasmonic hot spots appear. Adding trace amount of Au^{3+} into the nanodisk colloid generates small-diameter nanorings (plasmonic hot spots). However, addition of excess amount of Au^{3+} yields large-diameter nanorings.

value, which is also called Purcell effect.[26] When the resonance interaction between exciton and plasmon is larger than their decay rates, strong coupling occurs between exciton and plasmon, and hence two new hybrid modes (plexcitons) separated by the characteristic Rabi splitting energy are formed.[27] Until now, plasmonic metal nanostructures with a variety of shapes such as core−shell nanoparticles,[27,28] nanoprisms,[29−31] nanorods,[32] nanoparticle dimers,[33] and recently nanodisks[10] have been used to observe plasmon−exciton hybrid states. In a recent study, a hollow gold nanoprism was used to observe strong coupling in the hollow gold nanoprism and J-aggregate dye.[34] However, the reported Rabi splitting energies are around 200 meV, and the transparency dip at the resonance condition is heavily damped because of the interband transitions in gold. Here, we report for the first time, colloidal synthesis of bimetallic circular-shaped plexcitonic nanorings with tunable properties, Figure 1. Different from the previous studies, the present work has the following main advantages: (i) colloidal synthesis of bimetallic plasmonic nanorings, (ii) demonstration of nanocavities or plasmonic hot spots in nanodisks, (iii) colloidal synthesis of nanoring-shaped plexcitonic nanoparticles, and (iv) controlling the onset of strong coupling by galvanic replacement reactions.

METHODS

Chemicals. Poly(sodium 4-styrenesulfonate) (PSS), $NaBH_4$, $AgNO_3$, trisodium citrate, ascorbic acid, and $HAuCl_4$ were purchased from Sigma-Aldrich and used without any further purification. 5,5′,6,6′-tetrachlorodi(4-sulfobutyl)-benzimidazolocarbocyanine (TDBC) dye was purchased from FEW Chemicals GmbH and used as received. In all of the reactions and preparations, Milli-Q water with a resistivity of 18.2 MΩ cm was used.

Synthesis of Silver Seeds. Isotropic, spherical silver nanoparticles were used as seeds in the synthesis of anisotropic silver nanoprisms.[29,30] Typically, silver seeds were prepared by using the following protocol. Trisodium citrate solution (5 mL, 2.5 mM) was loaded in a plastic vial. After this, 0.25 mL of PSS (500 mg/L) and 0.3 mL of freshly prepared $NaBH_4$ (10 mM) were added to trisodium citrate solution. Subsequently, 5 mL of 0.5 mM $AgNO_3$ solution was added dropwise with a rate of ∼2 mL/min to the mixture described above under magnetic stirring. Appearance of yellow color after around half an hour and strong extinction peak at around 400 nm are strong indications of spherical silver nanoparticle colloid formation. Then, seed solution was aged for about 2 h for decomposing excess boron hydride, and consequently, the yellow-colored seed colloid was obtained.

Synthesis of Silver Nanoprisms and Nanodisks. Silver nanodisks were synthesized through a seed-mediated growth process described in detail in our previous work.[10] First, 5 mL of Millipore water was loaded in a plastic vial. Then, 75 μL of 10 mM ascorbic acid and various amount of seed solution (60, 100, and 150 μL) were added to the vial. Subsequently, 3 mL of 0.5 mM $AgNO_3$ solution was added dropwise with a rate of ∼1 mL/min into the solution mixture under stirring. The obtained silver nanoprism colloid was stabilized with the addition of 0.5 mL of 25 mM trisodium citrate solution, and then the colloid was aged for around half an hour. In this way, plasmon resonance wavelength of the nanoprisms can be tuned from 400 nm to more than 1100 nm. In order to provide morphological evolution from the nanoprism to nanodisk, the obtained silver nanoprism colloid was placed in an oil bath at 95 °C and magnetically stirred for around 2 h. After 2 h, the silver nanodisk colloid was cooled down to room temperature with quenching in water and then stored in the dark for further use.

Synthesis of Silver−Gold-Alloyed Nanorings. In order to synthesize plasmonic nanorings, first, the silver nanodisk colloid was synthesized. Immediately thereafter, 0.5 mL of 5 mg/L $HAuCl_4$ solution was injected into the silver nanodisk colloid for several times (between 4 and 18 times) with 2 min time intervals for obtaining silver−gold-alloyed nanorings. Increasing the total amount of $HAuCl_4$ injected into the silver nanodisk colloid resulted in the hollow site in silver−gold alloy nanorings. Further, silver−gold-alloyed nanorings were centrifuged at 15,000 rpm for 10 min. Supernatant was discarded, and the precipitate was redispersed in water. This procedure was applied several times until all the reaction byproducts were totally removed.

Synthesis of Plexcitonic Nanorings. Plexcitonic nanorings were synthesized by mixing 1 mL of alloyed nanoring colloid with varying amounts of 0.1 mM TDBC dye.[29]

https://dx.doi.org/10.1021/acs.jpcc.0c01011
J. Phys. Chem. C 2020, 124, 8334−8340

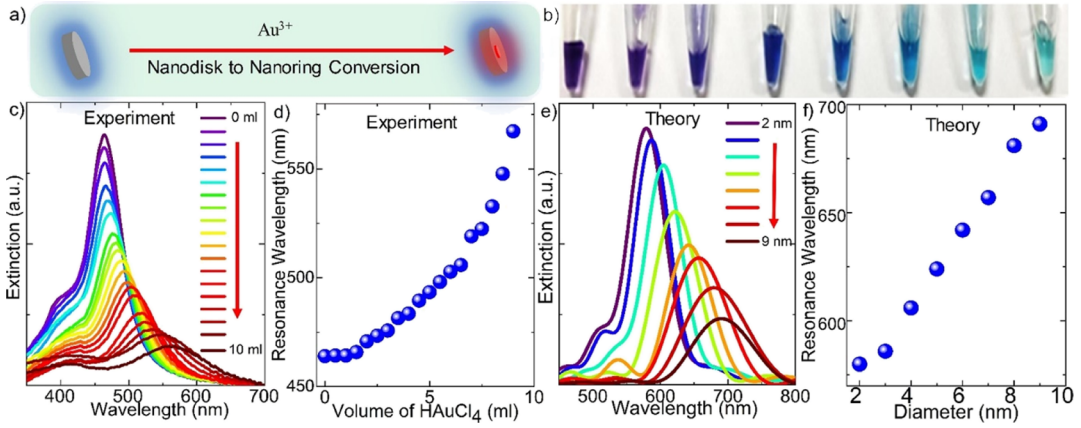

Figure 2. Tuning plasmon resonance by galvanic replacement reaction. (a) Schematic representation of conversion of nanodisks into nanorings. (b) Photo of silver nanodisk colloid treated with varying amounts of gold ions. (c,d) Experimental extinction spectra of silver nanodisk colloid upon addition of varying amounts of gold ions and corresponding plasmon resonance wavelength shift. (e,f) Calculated extinction spectra of plasmonic nanodisk with a central nanohole for varying nanohole diameter, that is, from 2 to 10 nm.

Thereafter, obtained solution was centrifuged at 15,000 rpm for 10 min. The supernatant was discarded for removing uncoupled dye molecules, and the precipitate was dispersed in water. The nanodisk- and nanoring-shaped plexcitonic nanoparticles shown in this study do not contain any uncoupled dye molecules in the colloid.

Characterization. Scanning transmission electron microscopy (STEM) was used in order to investigate morphological evolution of nanocrystals (SEM; Quanta 250, FEI, Hillsboro, OR, USA). The STEM detector was also attached to SEM Quanta. The electron beam energy was 15 kV, and the spot size was 2.5. The working distance was set at 5.3 mm. The microscope can be used in bright- and dark-field contrast modes independently. The samples were prepared by drop-casting nanocrystal suspensions onto the 200 mesh carbon-coated copper grid. Extinction measurements of colloids in the aqueous environment were performed by using a balanced deuterium–tungsten halogen light source (DH2000-BAL, Ocean Optics) and a fiber-coupled spectrometer (USB4000, Ocean Optics). All the characterization measurements were performed at room temperature.

Numerical Calculations. The finite difference time domain (FDTD) method was employed to explore optical properties of bare and coupled plasmonic nanoparticles by using a commercial FDTD package from Lumerical (see also Supporting Information). The plasmon–exciton coupling regimes in J-aggregate-coated silver and silver–gold-alloyed nanoparticles were extensively investigated from the weak to strong coupling regimes. It should be noted here that silver–gold-alloyed nanoring diameter and nanoring thickness were deduced from the STEM images. In FDTD simulations, the electric field polarization is along the x-axis, and the plane wave moves in the z-axis. The mesh size is 1 nm during the extinction spectra simulations and 0.1 nm during the electric field map simulations.

RESULTS AND DISCUSSION

General synthesis procedure of nanoring-shaped plexcitonic nanoparticles is displayed in Figure 1. Isotropic, spherical silver nanoparticles synthesized in aqueous medium were employed as seeds in the synthesis of anisotropic silver nanoprisms.[10] The number of seed nanoparticles in the reaction medium directly determines the final edge length of the nanoprism and hence localized SPP resonance wavelength. The anisotropic silver and gold nanoparticles have dipole plasmon resonance, which can be effectively tuned by changing the size and shape of the nanoparticle.[35] Silver nanodisks were synthesized through a seed-mediated growth process described in detail in our previous work.[30] The shape conversion of silver nanoprisms to nanodisks through heating was accomplished by placing the nanoprism colloid in an oil bath.[10]

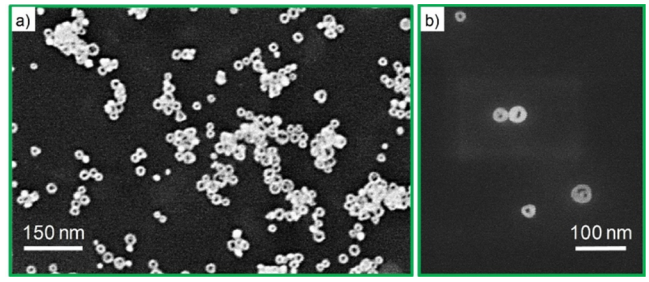

Figure 3. Plasmonic nanorings. (a) STEM image of nanorings synthesized by adding excess amount of gold ions into the silver nanodisk colloid. (b) Addition of trace amount of gold ions into the silver nanodisk colloid generates nanoholes on the nanodisks.

In order to synthesize hollow metal nanoparticles, we used galvanic replacement reactions, Figure 2a. A schematic representation represents conversion of nanodisks into nanorings. Previously, these reactions were used for the synthesis of gold and silver nanoframes, nanocages, and nanoboxes.[21,24] Galvanic replacement reaction involves an electrochemical reaction between silver and gold, owing to the difference in their standard electrochemical reduction potentials.

$$Au^{3+} + 3Ag \rightarrow Au + 3Ag^{+} \qquad \Delta E^{o} = +0.7\ V$$

The silver atoms on the silver nanodisks are oxidized, and gold ions in the solution are reduced in the vicinity of silver atoms. The reaction between gold ions and silver atoms in the nanodisk is spontaneous because the free energy of the above reaction, $\Delta G^{o} = -nFE^{o}$, where n is the number of electrons, F is the Faraday constant, and E^{o} is the standard cell potential of the reaction, is negative.[36] Additionally, each gold ion replaces three silver atoms in the nanoparticle, and hence the silver nanodisk is hollowed out by the electrochemical reaction. Remarkably, the amount of gold ions in the reaction medium effectively controls the size of the nanoholes.

https://dx.doi.org/10.1021/acs.jpcc.0c01011
J. Phys. Chem. C 2020, 124, 8334–8340

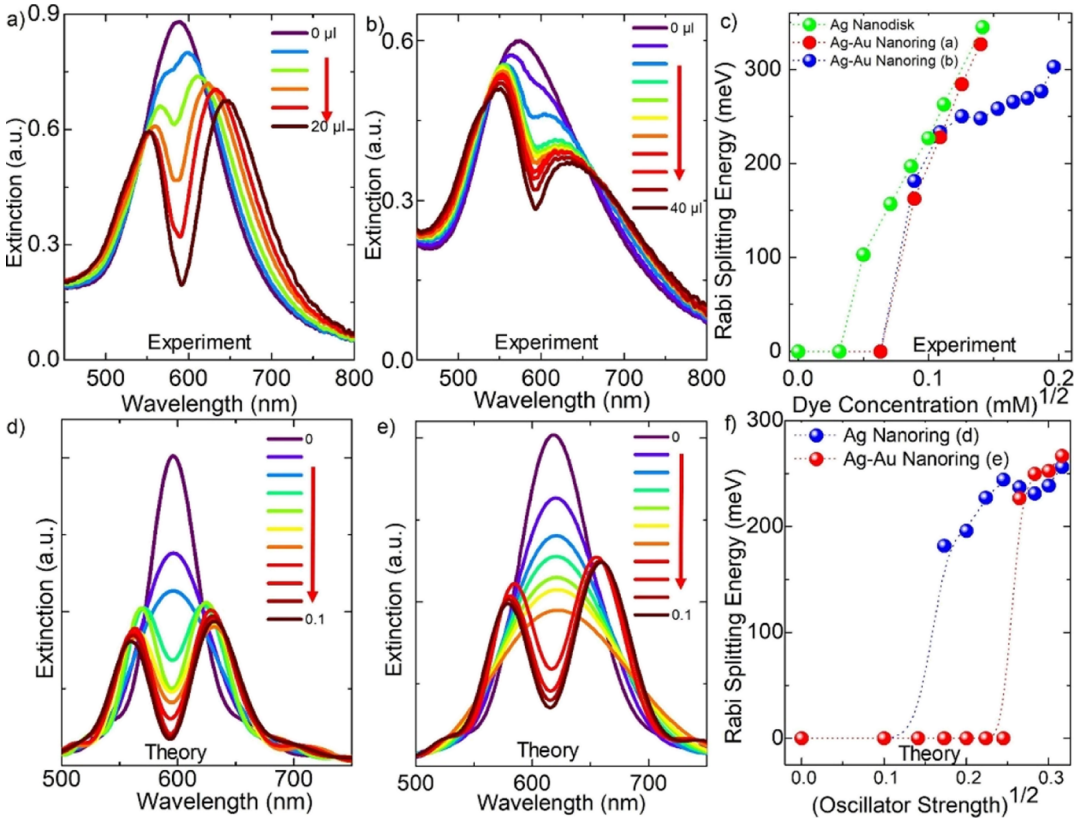

Figure 4. Tunable Rabi splitting energy in nanoring-shaped plexcitonic nanoparticles. The extinction spectra of plexcitonic nanoparticles with varying amount of J-aggregate dye added to the nanoring colloid containing (a) small nanoholes and (b) large nanoholes. Owing to the presence of larger amount of gold in (b), the extinction curves shown in (b) indicate very clear interband transitions of gold. (c) Rabi splitting energies as a function of square root of dye concentration calculated from the extinction spectra shown in (a,b). Theoretically calculated extinction spectra of a nanoring-shaped plexcitonic nanoparticle as a function of dye oscillator strength for (d) a silver nanoring and (e) a silver−gold nanoring. (f) Rabi splitting energies as a function of square root of oscillator strength of the dye.

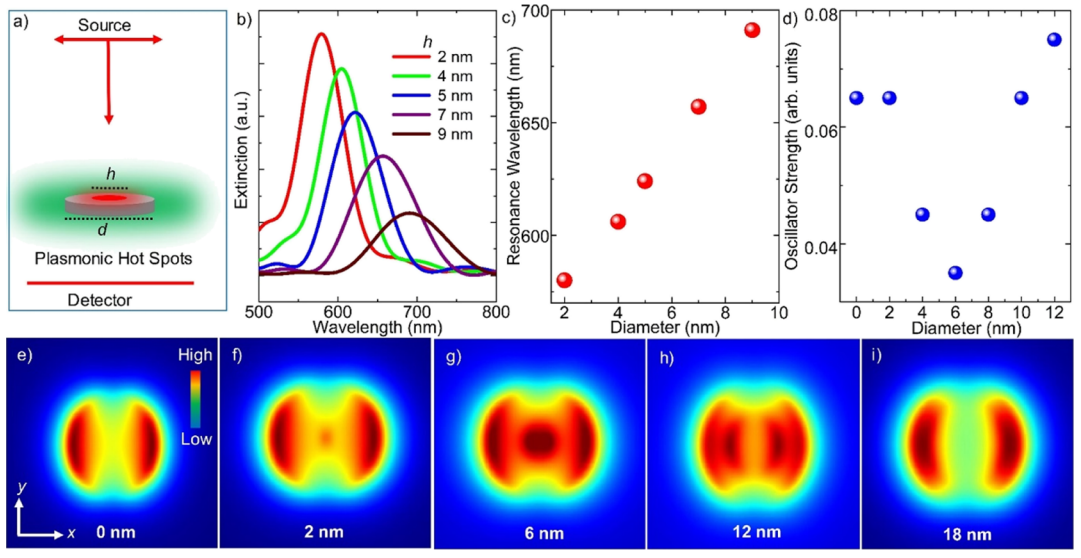

Figure 5. Numerical calculation of a nanoring. (a) Schematic representation of simulation of a nanoring with a central hole. (b,c) The curves from left to right represent theoretically calculated extinction spectra for a nanohole diameter ranging from 2 to 9 nm. (d) Onset of the transition from weak to strong coupling for a nanohole diameter ranging from 0 to 12 nm. (e−i) Electric field distribution of a single nanoring at resonance wavelength with varying inner diameter ranging from 0 to 18 nm.

In order to synthesize the bimetallic nanoring, first, the silver nanodisk colloid was synthesized. We injected various quantities of $HAuCl_4$ solution into the silver nanodisk colloid and traced the extinction spectra of the colloid, Figure 2b−d. The color variation of the colloid is shown in Figure 2b. The origin of plasmon resonance redshift upon addition of gold ions is ascribed to the coupling of dipolar modes at the inner and outer surfaces of the nanoring.[13] The plasmon resonance wavelength

https://dx.doi.org/10.1021/acs.jpcc.0c01011
J. Phys. Chem. C 2020, 124, 8334−8340

of the colloid is tuned more than 100 nm in Figure 2c. A careful analysis of the extinction spectra shown in Figure 2c,e reveals that the quality factor of the plasmon resonance decreases with the increase in the inner diameter of the nanoring. The quality factor of the plasmon resonance of the plasmonic cavity representing the degree of damping in the plasmonic cavity can be calculated as $Q = w_c/\gamma$, the ratio of the plasmon resonance frequency to the cavity damping, where w_c is the resonance frequency, and γ is the damping rate. Therefore, as the size of the nanohole increases, plasmon damping in the plasmonic cavity increases. Besides, we performed numerical calculations of the nanorings. The size of the nanohole is varied from 2 to 10 nm. In fact, compared to the silver nanodisk, the bimetallic nanoring represents a red-shifted plasmon resonance that can be tuned over an extended wavelength range by simply changing the ring inner diameter. Actually, the experimentally observed wavelength variation shown in Figure 2c,d is qualitatively well reproduced by theoretical calculations in Figure 2e,f.

STEM images and energy-dispersive X-ray (EDX) elemental analysis show that silver−gold nanorings are formed. Addition of excess amounts of gold ions yielded silver−gold nanorings, Figure 3a. On the other hand, addition of trace amounts of gold ions yielded very small nanoholes on the nanodisks, Figure 3b. Most of the nanorings are in circular shape, and nearly all of the nanodisks are drilled by the gold ions, see the Supporting Information for the large-area STEM image of nanorings. Besides, EDX spectra confirmed the presence of silver and gold in the bimetallic nanoparticles, see the Supporting Information.

Plexcitonic nanorings were synthesized by self-assembly of J-aggregate dyes on bimetallic nanorings.[29] In the strong coupling regime, plasmons and excitons interact strongly, and consequently, new hybrid polariton modes are formed. By using the coupled oscillator model, the energies of the upper and lower polariton branches can be represented as $E_{1,2} = (E_p + E_{ex})/2 \pm 1/2\ ((4g^2 + (E_p - E_{ex})^2))^{1/2}$, where E_1 and E_2 are the upper and lower polariton energies, g is the coupling strength, and E_p and E_{ex} are the plasmon and exciton resonance energies.[37] At zero detuning, the energy difference between the upper and lower polariton branches is called Rabi splitting energy defined as $\Delta E = E_2 - E_1 = \hbar\Omega = 2g$, where g is the coupling strength. Including plasmon damping rate, γ_p, and exciton damping rate, γ_{ex}, the Rabi splitting is now $\hbar\Omega = 4g^2 + (\gamma_p - \gamma_{ex})^2$. Strong coupling occurs when coupling strength, g, is at least larger than $(\gamma_p - \gamma_{ex})/2$. In order to tune coupling strength, we added various quantities of J-aggregate dyes into the nanoring colloid and extensively analyzed the extinction spectra of the hybrid system, Figure 4a−c. In Figure 4b, the amount of gold ions added to silver nanodisk is larger than the one in Figure 4a. Owing to the presence of a larger amount of gold in Figure 4b, the extinction curves indicate very clear interband transition in gold. It is worth noting that the calculated and experimentally observed interband edge of gold is at around 2.38 eV.[38] The calculated Rabi splitting energies as a function of the square root of dye concentration are displayed in Figure 4c. Theoretically calculated extinction spectra of the plexcitonic nanoparticle for a silver nanoring and for a silver−gold alloyed nanoring are shown in Figure 4d,e, respectively. The calculated Rabi splitting energies from theoretically obtained curves are indicated in Figure 4f. It should be pointed out here that Rabi splitting energy, $\hbar\Omega \approx (f_0)^{1/2}$, depends on the oscillator strength, f_0, of the exciton. The experimental and theoretical results shown in Figure 4 clearly demonstrate that transition from weak coupling to strong coupling regime can be controlled by gold.

Theoretical calculations further support that plasmonic hot spots can be generated in bimetallic nanorings by adjusting the inner diameter of the nanoring, Figure 5. In addition, the onset of the strong coupling is lowered at the plasmonic hot spots. The schematic representation depicts a single nanoring with varying inner diameter size, Figure 5a. The spectra shift to longer wavelengths with an increase in the diameter of the nanohole, Figure 5b,c. Owing to the plasmonic hot spot formation at 6 nm nanohole diameter, the onset of the transition from weak to strong coupling is the lowest for a 6 nm nanohole diameter, Figure 5d. Indeed, the electric field intensity and localization in the nanohole are the largest for a nanohole of 6 nm, Figure 5d−h. Because the coupling strength (g), $\hbar\Omega = 2g - 1/(V)^{1/2}$, is proportional to the effective mode volume of the cavity, V, we expect to see large enhancement in light matter interaction in plasmonic nanocavities. Therefore, the nanoholes (∼6 nm) drilled in nanodisks by gold ions are indeed plasmonic nanocavities.

CONCLUSIONS

In summary, we have demonstrated for the first time that colloidal bimetallic nanorings with plasmonic hot spots and tunable plasmon resonance wavelengths in the visible spectrum can be synthesized by galvanic replacement reactions. The size of the inner diameter of the nanoring can be controlled by the amount of gold ions introduced in the galvanic replacement reaction. The nanorings with small holes produce plasmonic hot spots (plasmonic nanocavities). Furthermore, we have shown for the first time that J-aggregate dyes self-assemble on the bimetallic nanorings, and hence nanoring-shaped plexcitonic nanoparticles are formed. The results reveal that the onset of strong coupling can be tamed by the galvanic displacement reactions. Theoretical calculations reveal that transition from weak coupling to strong coupling is lowered for the 6 nm-diameter nanohole. Furthermore, the space enclosed by plasmonic nanocavities on silver nanodisks is empty and hence accessible to a variety of molecules, ions, and quantum dots for sensing and spectroscopy applications at the nanometer scale.[5]

ASSOCIATED CONTENT

Supporting Information

The Supporting Information is available free of charge at https://pubs.acs.org/doi/10.1021/acs.jpcc.0c01011.

STEM image of plasmonic nanorings, EDX analysis of silver−gold nanorings, tuning color of silver nanodisk by galvanic replacement reaction, extinction spectra of nanodisk shaped plasmonic and plexcitonic nanoparticles, numerical calculations of nanoring shaped plasmonic and plexcitonic nanoparticles, imaginary and real parts of the dielectric function of Lorentz oscillator, and absorbance spectrum of J-aggregate (PDF)

AUTHOR INFORMATION

Corresponding Author

Sinan Balci − *Department of Photonics, Izmir Institute of Technology, 35430 Izmir, Turkey;* orcid.org/0000-0002-9809-8688; Email: sinanbalci@iyte.edu.tr

Authors

C. Meric Guvenc − *Department of Materials Science and Engineering, Izmir Institute of Technology, 35430 Izmir, Turkey*

https://dx.doi.org/10.1021/acs.jpcc.0c01011
J. Phys. Chem. C 2020, 124, 8334−8340

Fadime Mert Balci − *Department of Photonics, Izmir Institute of Technology, 35430 Izmir, Turkey*
Sema Sarisozen − *Department of Chemistry, Izmir Institute of Technology, 35430 Izmir, Turkey*
Nahit Polat − *Department of Photonics, Izmir Institute of Technology, 35430 Izmir, Turkey*

Complete contact information is available at: https://pubs.acs.org/10.1021/acs.jpcc.0c01011

Notes

The authors declare no competing financial interest.

■ ACKNOWLEDGMENTS

This research was supported by TUBITAK (118F066 and 117F172).

■ REFERENCES

(1) Barnes, W. L.; Dereux, A.; Ebbesen, T. W. Surface Plasmon Subwavelength Optics. *Nature* **2003**, *424*, 824−830.
(2) Grésillon, S.; Aigouy, L.; Boccara, A. C.; Rivoal, J. C.; Quelin, X.; Desmarest, C.; Gadenne, P.; Shubin, V. A.; Sarychev, A. K.; Shalaev, V. M. Experimental Observation of Localized Optical Excitations in Random Metal-Dielectric Films. *Phys. Rev. Lett.* **1999**, *82*, 4520−4523.
(3) Bek, A.; Jansen, R.; Ringler, M.; Mayilo, S.; Klar, T. A.; Feldmann, J. Fluorescence Enhancement in Hot Spots of AFM-Designed Gold Nanoparticle Sandwiches. *Nano Lett.* **2008**, *8*, 485−490.
(4) Xu, H.; Bjerneld, E. J.; Käll, M.; Börjesson, L. Spectroscopy of Single Hemoglobin Molecules by Surface Enhanced Raman Scattering. *Phys. Rev. Lett.* **1999**, *83*, 4357−4360.
(5) Chikkaraddy, R.; de Nijs, B.; Benz, F.; Barrow, S. J.; Scherman, O. A.; Rosta, E.; Demetriadou, A.; Fox, P.; Hess, O.; Baumberg, J. J. Single-Molecule Strong Coupling at Room Temperature in Plasmonic Nanocavities. *Nature* **2016**, *535*, 127−130.
(6) Xia, Y.; Xiong, Y.; Lim, B.; Skrabalak, S. E. Shape-Controlled Synthesis of Metal Nanocrystals: Simple Chemistry Meets Complex Physics? *Angew. Chem., Int. Ed. Engl.* **2009**, *48*, 60−103.
(7) Murphy, C. J. Nanocubes and Nanoboxes. *Science* **2002**, *298*, 2139−2141.
(8) Sherry, L. J.; Jin, R.; Mirkin, C. A.; Schatz, G. C.; Van Duyne, R. P. Localized Surface Plasmon Resonance Spectroscopy of Single Silver Triangular Nanoprisms. *Nano Lett.* **2006**, *6*, 2060−2065.
(9) Yu, Y. Y.; Chang, S.-S.; Lee, C.-L.; Wang, C. R. C. Gold Nanorods: Electrochemical Synthesis and Optical Properties. *J. Phys. Chem. B* **1997**, *101*, 6661−6664.
(10) Balci, F. M.; Sarisozen, S.; Polat, N.; Balci, S. Colloidal Nanodisk Shaped Plexcitonic Nanoparticles with Large Rabi Splitting Energies. *J. Phys. Chem. C* **2019**, *123*, 26571−26576.
(11) Lee, S.-M.; Jun, Y.-w.; Cho, S.-N.; Cheon, J. Single-Crystalline Star-Shaped Nanocrystals and Their Evolution: Programming the Geometry of Nano-Building Blocks. *J. Am. Chem. Soc.* **2002**, *124*, 11244−11245.
(12) Seo, D.; Song, H. Asymmetric Hollow Nanorod Formation through a Partial Galvanic Replacement Reaction. *J. Am. Chem. Soc.* **2009**, *131*, 18210−18211.
(13) Aizpurua, J.; Hanarp, P.; Sutherland, D. S.; Kall, M.; Bryant, G. W.; de Abajo, F. J. G. Optical Properties of Gold Nanorings. *Phys. Rev. Lett.* **2003**, *90*, 057401.
(14) Yang, P.; Zheng, J.; Xu, Y.; Zhang, Q.; Jiang, L. Colloidal Synthesis and Applications of Plasmonic Metal Nanoparticles. *Adv. Mater.* **2016**, *28*, 10508−10517.
(15) Lin, X.; Liu, Y.; Lin, M.; Zhang, Q.; Nie, Z. Synthesis of Circular and Triangular Gold Nanorings with Tunable Optical Properties. *Chem. Commun.* **2017**, *53*, 10765−10767.
(16) Ghosh, T.; Satpati, B.; Senapati, D. Characterization of Bimetallic Core-Shell Nanorings Synthesized Via Ascorbic Acid-Controlled Galvanic Displacement Followed by Epitaxial Growth. *J. Mater. Chem. C* **2014**, *2*, 2439−2447.
(17) Genç, A.; Patarroyo, J.; Sancho-Parramon, J.; Bastús, N. G.; Puntes, V.; Arbiol, J. Hollow Metal Nanostructures for Enhanced Plasmonics: Synthesis, Local Plasmonic Properties and Applications. *Nanophotonics* **2017**, *6*, 193−213.
(18) Tsai, C.-Y.; Lin, J.-W.; Wu, C.-Y.; Lin, P.-T.; Lu, T.-W.; Lee, P.-T. Plasmonic Coupling in Gold Nanoring Dimers: Observation of Coupled Bonding Mode. *Nano Lett.* **2012**, *12*, 1648−1654.
(19) Halpern, A. R.; Corn, R. M. Lithographically Patterned Electrodeposition of Gold, Silver, and Nickel Nanoring Arrays with Widely Tunable near-Infrared Plasmonic Resonances. *ACS Nano* **2013**, *7*, 1755−1762.
(20) Chow, T. H.; Lai, Y.; Cui, X.; Lu, W.; Zhuo, X.; Wang, J. Colloidal Gold Nanorings and Their Plasmon Coupling with Gold Nanospheres. *Small* **2019**, *15*, 1902608.
(21) Métraux, G. S.; Cao, Y. C.; Jin, R.; Mirkin, C. A. Triangular Nanoframes Made of Gold and Silver. *Nano Lett.* **2003**, *3*, 519−522.
(22) Krishnan, S. K.; Esparza, R.; Flores-Ruiz, F. J.; Padilla-Ortega, E.; Luna-Bárcenas, G.; Sanchez, I. C.; Pal, U. Seed-Mediated Growth of Ag@Au Nanodisks with Improved Chemical Stability and Surface-Enhanced Raman Scattering. *ACS Omega* **2018**, *3*, 12600−12608.
(23) McLellan, J. M.; Geissler, M.; Xia, Y. Edge Spreading Lithography and Its Application to the Fabrication of Mesoscopic Gold and Silver Rings. *J. Am. Chem. Soc.* **2004**, *126*, 10830−10831.
(24) Sun, Y.; Xia, Y. N. Shape-Controlled Synthesis of Gold and Silver Nanoparticles. *Science* **2002**, *298*, 2176−2179.
(25) Daniel, J. R.; McCarthy, L. A.; Ringe, E.; Boudreau, D. Enhanced Control of Plasmonic Properties of Silver-Gold Hollow Nanoparticles Via a Reduction-Assisted Galvanic Replacement Approach. *RSC Adv.* **2019**, *9*, 389−396.
(26) Purcell, E. M.; Torrey, H. C.; Pound, R. V. Resonance Absorption by Nuclear Magnetic Moments in a Solid. *Phys. Rev.* **1946**, *69*, 37−38.
(27) Fofang, N. T.; Park, T.-H.; Neumann, O.; Mirin, N. A.; Nordlander, P.; Halas, N. J. Plexcitonic Nanoparticles: Plasmon-Exciton Coupling in Nanoshell-J-Aggregate Complexes. *Nano Lett.* **2008**, *8*, 3481−3487.
(28) Wiederrecht, G. P.; Wurtz, G. A.; Hranisavljevic, J. Coherent Coupling of Molecular Excitons to Electronic Polarizations of Noble Metal Nanoparticles. *Nano Lett.* **2004**, *4*, 2121−2125.
(29) Balci, S. Ultrastrong Plasmon-Exciton Coupling in Metal Nanoprisms with J-Aggregates. *Opt. Lett.* **2013**, *38*, 4498−4501.
(30) Balci, S.; Kucukoz, B.; Balci, O.; Karatay, A.; Kocabas, C.; Yaglioglu, G. Tunable Plexcitonic Nanoparticles: A Model System for Studying Plasmon-Exciton Interaction from the Weak to the Ultrastrong Coupling Regime. *ACS Photonics* **2016**, *3*, 2010−2016.
(31) Wersäll, M.; Cuadra, J.; Antosiewicz, T. J.; Balci, S.; Shegai, T. Observation of Mode Splitting in Photoluminescence of Individual Plasmonic Nanoparticles Strongly Coupled to Molecular Excitons. *Nano Lett.* **2017**, *17*, 551−558.
(32) Beane, G.; Brown, B. S.; Johns, P.; Devkota, T.; Hartland, G. V. Strong Exciton-Plasmon Coupling in Silver Nanowire Nanocavities. *J. Phys. Chem. Lett.* **2018**, *9*, 1676−1681.
(33) Pérez-González, O.; Zabala, N.; Aizpurua, J. Optical Properties and Sensing in Plexcitonic Nanocavities: From Simple Molecular Linkers to Molecular Aggregate Layers. *Nanotechnology* **2013**, *25*, 035201.
(34) Das, K.; Hazra, B.; Chandra, M. Exploring the Coherent Interaction in a Hybrid System of Hollow Gold Nanoprisms and Cyanine Dye J-Aggregates: Role of Plasmon-Hybridization Mediated Local Electric-Field Enhancement. *Phys. Chem. Chem. Phys.* **2017**, *19*, 27997−28005.
(35) Kelly, K. L.; Coronado, E.; Zhao, L. L.; Schatz, G. C. The Optical Properties of Metal Nanoparticles: The Influence of Size, Shape, and Dielectric Environment. *J. Phys. Chem. B* **2003**, *107*, 668−677.
(36) Swaddle, T. W. *Inorganic Chemistry: An Industrial and Environmental Perspective*; Academic Press: San Diego, 1997.
(37) Balci, S.; Kocabas, C.; Ates, S.; Karademir, E.; Salihoglu, O.; Aydinli, A. Tuning Surface Plasmon-Exciton Coupling Via Thickness Dependent Plasmon Damping. *Phys. Rev. B: Condens. Matter Mater. Phys.* **2012**, *86*, 235402.

(38) Christensen, N. E.; Seraphin, B. O. Relativistic Band Calculation and the Optical Properties of Gold. *Phys. Rev. B: Solid State* **1971**, *4*, 3321−3344.

https://dx.doi.org/10.1021/acs.jpcc.0c01011
J. Phys. Chem. C 2020, 124, 8334−8340